

Fabrication and Characterization of Glycerol/Chitosan/Polyvinyl Alcohol-Based Transparent Hydrogel Films Loaded with Silver Nanoparticles for Antibacterial Wound Dressing Applications

Abstract

Background: Wounds have a bad prognostic nature and excessive discharges whose regular wound dressings are ineffective. Hydrogels are the best candidates for dressing such wounds due to their high water content and ability to exchange substances. Accordingly, the purpose of this study was to make a novel hydrogel wound dressing following the integration of various findings on wound healing and the use of regenerative medicine. **Materials and Methods:** Various compounds were fabricated by glycerol/chitosan/polyvinyl alcohol (PVA) and then characterized to obtain the optimal composition using several techniques, including a water vapor passage test, scanning electron microscopy, water absorption, tensile strength, biodegradability, Fourier transform infrared spectroscopy, and antibacterial test. **Results:** The findings revealed the optimal dressing ratio. Better antibacterial activity was found for the silver nanoparticle (AgNP) dressing. **Conclusion:** Our new fabricated dressing, glycerol/chitosan/PVA hydrogel loaded with AgNPs, exhibited satisfactory wound healing properties.

Keywords: Anti-bacterial agents, chitosan, glycerol, polyvinyl alcohol, metal nanoparticles, tissue engineering, wound healings bandages

Introduction

The skin is the largest organ of the body and is composed of two layers. The superficial (the epidermis) is composed of the keratinized, stratified squamous epithelium; the deep layer (the dermis) contains dense connective tissue, blood vessels, and collagen fibers.^[1]

The term “wound” refers to a rupture or injury to the epidermis, dermis, or both; wounds can occur following trauma or pathological changes to the skin or body.^[2]

Wounds can affect the structure and function of the skin. Wounds can affect the structure and function of the skin. There are various types of wounds including chronic wounds, diabetic wounds, surgical wounds, and tears and burns that are more common than the others. When an area of more than 0.5 square inches is lost from the surface of the skin, grafting is necessary to regenerate the skin.^[3,4]

Contrary to the common belief that keeping wounds dry equals to faster healing, in 1962, Dr. Winter proved that wound healing

was much faster when a moist dressing was applied. Wet dressing facilitates cell migration and autolytic debridement besides stimulating both fibroblasts to secrete collagen and macrophages. Moreover, it forms a suitable substrate for the transfer of enzymes and hormones such as growth hormones.^[5,6]

Dressings are generally divided into conventional and modern types. Some conventional dressings are wool yarn, natural or synthetic bandages, and gauze, while some modern dressings include hydrocolloids, alginate, hydrogel, semi-permeable membranes, adhesive films, BioFoam dressings, and tissue-engineered skin substitutes. Modern dressings not only cover the wound but also promote the wound healing process.^[6,7]

Hydrogels are three-dimensional networks of hydrophilic polymers with extraordinary fluid uptake capacity. These compounds can absorb water (up to a thousand times the weight of polymer) without dissolving. Compared to other synthetic materials,

Ali Samadi^{1,2},
Saeed Azandeh^{1,2},
Mahmoud
Orazizadeh^{1,2},
Vahid Bayati^{1,2},
Mohammad
Rafienia³,
Masoud Ali Karami⁴

¹Cellular and Molecular
Research Center, Ahvaz

Jundishapur University of
Medical Sciences, Ahvaz,

²Department of Anatomical
Sciences, School of Medicine,
Ahvaz Jundishapur University
of Medical Sciences, Ahvaz,

³Biosensor Research Center;

Isfahan University of Medical

Sciences, Isfahan, ⁴Department

of Pharmaceutics, School of

Pharmacy, Ahvaz Jundishapur

University of Medical Sciences,

Ahvaz, Iran

Address for correspondence:

Dr. Saeed Azandeh,

Department of Anatomical

Sciences, Ahvaz Jundishapur

University of Medical Sciences,

Faculty of Medicine, Ahvaz,

Iran.

E-mail: azandeh-s@ajums.ac.ir

Received: 01 September 2020

Revised: 03 October 2020

Accepted: 24 October 2020

Published: 27 January 2021

Access this article online

Website: www.advbiores.net

DOI: 10.4103/abr.abr_211_20

Quick Response Code:



How to cite this article: Samadi A, Azandeh S, Orazizadeh M, Bayati V, Rafienia M, Karami MA. Fabrication and characterization of glycerol/chitosan/polyvinyl alcohol-based transparent hydrogel films loaded with silver nanoparticles for antibacterial wound dressing applications. Adv Biomed Res 2021;10:4.

This is an open access journal, and articles are distributed under the terms of the Creative Commons Attribution-NonCommercial-ShareAlike 4.0 License, which allows others to remix, tweak, and build upon the work non-commercially, as long as appropriate credit is given and the new creations are licensed under the identical terms.

For reprints contact: WKHLRPMedknow_reprints@wolterskluwer.com

hydrogels have a soft and elastic surface, whose physical and chemical properties are similar to living tissues.^[8]

The hydrogels based on chitosan and polyvinyl alcohol (PVA) are of particular interest not only because of their incredible physical, chemical, and biological properties – high biocompatibility, controlled biodegradation, cooling, and moisturizing properties for treating burn wounds, but their potential in drug delivery applications. Moreover, the chitosan-PVA-based hydrogels can absorb the wound exudate effectively, which is their superiority over other materials available for dressing applications.^[8,9]

Silver nanoparticles (AgNPs) are among the most widely used products in biomedical applications, as their antimicrobial properties have been proven for years and can eliminate more than 650 species of bacteria, viruses, and fungi. Importantly, the target bacteria do not resist these particles. As a result, AgNPs are effective in eliminating a wide range of microorganisms. In addition to bacteria, AgNPs bind to glycoproteins on the surface of the virus and eventually killing it.^[10-12]

Materials and Methods

Materials

Silver nitrate, chitosan (COS, 90% deacetylated, Mn = 550, polydispersity index = 1.06), and PVA were provided by Sigma-Aldrich Chemicals Company, Germany. Glycerol was provided by Merck Chemicals Company-Germany. DMEM high glucose and fetal bovine serum (FBS) was provided by Gibco Biological Company, Island. Other reagents were purchased from Merck (Germany).

Synthesis of silver nanoparticles

3.37 mg (2.002 mmole) of silver nitrate was dissolved in 30 ml of pure ethanol. After 20 min, the size of the soluble nanoparticles reached 30 nm, and they were subsequently used to prepare the dressing.^[13]

Fabrication of glycerol/chitosan/polyvinyl alcohol films and selection of optimal ratio for use in dressing

20 mg/mL solutions of chitosan were made in acetic acid 1% and 10 mg/mL of PVA in Milli-Q water. Glycerol was used as a film plasticizer. The composite films were fabricated through casting technique [Table 1] to determine the optimal ratio of components. The photography was applied to show if the difference in component percentages affected the film optical transparency.

The physical and chemical properties of samples were analyzed through scanning electron microscopy (SEM), tensile strength tests, Fourier transform infrared spectroscopy (FTIR), biodegradability, water vapor transmission rate (WVTR), and water absorption (WA). A cell viability test was performed to evaluate the cell compatibility of samples.

Table 1: Samples of fabricated composite films

Sample name	Chitosan (% v/v)	PVA (% v/v)	Glycerol (% v/v)	Nanosilver (mmole)
C40	38	58	4	0
C50	48	48	4	0
C50s	48	48	4	2.002
C60	58	38	4	0
C80	78	18	4	0

PVA: Polyvinyl alcohol

Scanning electron microscopy

After drying, the samples were cut into 1 cm × 1 cm and mounted onto a clean slide. The surfaces of samples were then coated with a gold layer to create the appropriate image resolution and transferred to the SEM chamber (LEO 1450VP, ZEISS, Berlin, Germany). The micrographs were taken at a voltage of 20 kv.

Mechanical test

The mechanical properties were measured according to ASTM D882-10 standards using a material testing machine (100 kN Automatic, WANCE, China). The strips were cut to a length of 50 mm and a width of 20 mm, and the thickness of each strip was measured. Then, the strips were placed in the device's panes. The device was fixed at 60 N load cell, and the panes were distanced at a speed of 10 mm/min to tear the sample ($n = 3$).

Attenuated total reflection

Due to the high reflective properties of films, the FTIR test could not be applied, and so the attenuated total reflection (ATR)-FTIR (Lasco 6300, JASCO, Pfungstadt, Germany) technique was applied instead. For preparation, the samples were cut into 2 cm² pieces, mounted on a clean slide and placed in the sample container compartment. The applied wavenumber was in the range of 400–3500 cm⁻¹ and a resolution of 4 cm⁻¹ to examine the functional groups and bonds in the molecules.

Biodegradability

In order to measure the percentage of weight loss (or biodegradability) of the samples, the first step was to measure the initial dry weight of each sample with a precise scale (HT 224, Intell-Lab, Tokyo, Japan). Then, each sample was immersed in phosphate-buffered saline (PBS). At specific intervals, each sample was removed and dried at room temperature, and finally, its dry weight was measured. The percentage of weight loss (X) was calculated through Equation 1 as follows:

$$X = \frac{W_1 - W_2}{W_1} \times 100$$

Equation 1 – The formula for calculating the percentage of sample biodegradability

where W_1 is the initial weight and W_2 is the sample's weight after being immersed into PBS ($n = 3$).

Water vapor transmission rate

The hydrogel moisture permeability was determined by measuring the WVTR based on the ASTM standards.^[14]

From each sample, a circle with a diameter of 2 cm was cut and placed into double-distilled water for 1 h to become hydrogel. It was then placed on the opening of a test tube with a diameter of 1.6 cm containing 15 mL of double-distilled water. Two test tubes without a film cover were considered as the control. The weight of each test tube along with all its contents (including the water and lid) was measured, and the tubes were transferred to an incubator at 37°C and 40% humidity for 24 h. After 24 h, the weights of tubes and their contents were re-measured. WVTR was calculated according to Equation 2 as follows:

$$\text{WVTR (g/m}^2 \times \text{day)} = \frac{W_i - W_f}{A} \times 100$$

Equation 2 – The formula for calculating the WVTR of the sample

where W_i is the initial weight of test tube and its contents, W_f is the final weight of test tube, and A is the area of test tube lids surface ($n = 3$).^[15,16]

Water absorption

To measure the WA of the samples, first, the initial dry weight of each sample was measured, and then, each sample was immersed in a separate container in Milli-Q water. After 24 h, each sample was removed from the water; after drying the surface water with filter paper, the weight of the wet sample was calculated according to Equation 3 as follows:

$$\text{WA (\%)} = \frac{W_w - W_d}{W_d} \times 100$$

Equation 3 – The formula for calculating the WA rate of samples

where W_w is the weight of wet sample and W_d is the weight of dry sample ($n = 3$).^[17]

Cell viability

Before loading the samples ($n = 3$) into wells, the wells were rinsed with PBS and filled with ethanol (70%). After 24 h, the ethanol was drained and the wells were rinsed several times with PBS (for 10 min each time). After draining the wells, the plate was exposed to ultraviolet light for 1 h, and 3800 human dermal fibroblasts (FfK, Pasteur Institute, Tehran, Iran) in the third passage were added to each well. A volume of 1 mL of work culture medium containing 89% DMEM HG (D5796, Sigma-Aldrich, Taufkirchen, Germany), 1% pen-strep (P4333,

Sigma-Aldrich, Taufkirchen, Germany), and 10% FBS (S0615, Sigma-Aldrich, Taufkirchen, Germany) was added to each well, and the plates were transferred to the incubator with 5% CO₂. The test was performed on days 1, 5, 6, and 7 using the MTT kit (P5368, Sigma-Aldrich, Taufkirchen, Germany) according to the manufacturer's instructions.

Finally, 100 μ L of the culture medium from each well was transferred to a 96-well plate, and their optical densities were read by ELISA reader (MPR4, Hyperion, Roedermark, Germany) at 570 nm. Finally, the cell viability was calculated according to Equation 4 as follows:

$$\text{Cell viability (\%)} = \frac{\text{OD}_{\text{test}} - \text{OD}_{\text{blank}}}{\text{OD}_{\text{control}} - \text{OD}_{\text{blank}}} \times 100$$

Equation 4 – The formula for calculating the percentage of cell viability of samples ($n = 3$).

Antibacterial test

Using a template, the fabricated films were turned into disks with a diameter of 10 mm. *Staphylococcus aureus* (ATCC 29213) and *Bacillus cereus* (ATCC 27853) bacteria were purchased. A single colony was taken from the bacteria, and four-zone culture was performed on the plate to activate the bacteria. Next, the plates were placed in an incubator at 37°C for 24 h to allow the bacteria to grow. They were subsequently kept at 4°C. To maintain the bacterial viability, they were re-cultured every 20 days. Then, a single colony was taken from the activated bacteria by the loop and added to a test tube containing 5 ml of sterile distilled water to obtain a bacterial suspension with 0.5 McFarland turbidity standard (1.5×10^8 cfu/ml). Then, under the laminar flow hood, we took the bacterial suspension from the test tube with a sterile swab. This process was followed by culturing by a lawn culture method. The discs were then normally seeded onto the Mueller-Hinton agar medium (Sigma-Aldrich, Germany) using forceps. The plates were incubated at 37°C for 24 h. Next, the diameter of the zone of inhibition (ZOI) was considered as an indicator of antimicrobial activity ($n = 3$).^[18,19]

Statistical analysis

The mean differences of the continuous data were analyzed by SPSS version 16 (SPSS Inc., Chicago, IL, USA) using a one-way analysis of variance and Tukey's *post hoc* test. All empirical data are shown as means \pm standard deviation. All tests were performed in triplicate. The significance level was $P < 0.05$.

Results

Optical transparency

The dressing transparency allows the wound healing process to be followed without the need for replacement.

Figure 1a shows the photographic images of the samples of the prepared films and compares the quality of their transparency with their control (i.e., the image of the university logo). All the fabricated films are transparent, and the logo on the back is clearly recognizable. However, the C50s, which contain AgNPs, are a bit opaquer (all specimens are 3 mm thick).

Scanning electron microscopy

At a magnification of $\times 2000$ and a voltage of 20,000 V [Figure 1b], the smooth and uniform surface of the composite film is easily visible. As the magnification increases to $\times 5000$ and the microscope focuses, many cracks are observed because of the bombardment of the surface of the films produced by the electrons released from the electron microscope cathode and their contact on the surface of the samples [Figure 1c]. The increase in the temperature of the sample due to the collision of electrons creates such a view that it shows an image of the appearance of a typical and flawless composite and proves that all the produced samples of polymer composite are complete and correct, which, in turn, shows the uniform composition in the composite [the image of all the samples was similar to Figure 1c].

Mechanical test

In this test, the silver-free samples were compared first [Figure 2a]. Their stress–strain curves and Young's modulus (C40 = 16.19814 MPa, C50 = 10.29646 MPa, C60 = 14.87413 MPa, and C80 = 8.921745 MPa) showed no significant difference in their mechanical strength, which was within the range of the mechanical properties of human skin (i.e., 0.2–20 MPa). However, with the addition of AgNPs to the composition of the composite film, it was

observed that the Young's modulus (C50s = 48.571427 MPa) of the film increased significantly while the tensile strength decreased slightly.

Attenuated total reflection

After testing and examining the shapes related to the samples [Figure 2b] and examining the relevant peaks, the presence of silver ions (1377 cm^{-1}) and silver metal (799 cm^{-1}) in the shape related to the sample C50s was confirmed. Peaks at 3295 cm^{-1} and 2930 cm^{-1} related to the redshift range of chitosan and PVA were also observed. The peak at 1029 cm^{-1} was related to vibrational bands of chitosan, and the rest of the peaks were related to PVA, which has OH, CH, C-O, C-C, and C = O bonds.^[20]

Biodegradability

The biodegradability test for samples determines whether the dressing produced is destroyed in the face of the environment and how long it will take if it is destroyed. Basically, the biodegradability test is important in tissue engineering products. According to Figure 3a, the biodegradability test for different samples was measured over 90 days. The results show that the C50s sample had significantly higher resistance to biodegradability than the other samples.

Water vapor transmission rate

The WVTR test shows the rate at which water vapor and gasses pass through the hydrogel dressing. According to Figure 3b, the WVTR is higher in all samples of produced films than in the control group, indicating that the fabricated film increases evaporation and is completely permeable to the passage of gasses. Different WVTR values were observed among different AgNP-free composite groups, which are probably related to the change of different composite ratios. However, the addition of AgNPs in the C50s ($4179\text{ g}/[\text{m}^2 \times \text{day}]$) group significantly increased WVTR compared to the C50s ($2702\text{ g}/[\text{m}^2 \times \text{day}]$) group, which has the same composition without AgNPs, and the control group that the test tube contains water without a film lid, as well as relative to other groups.

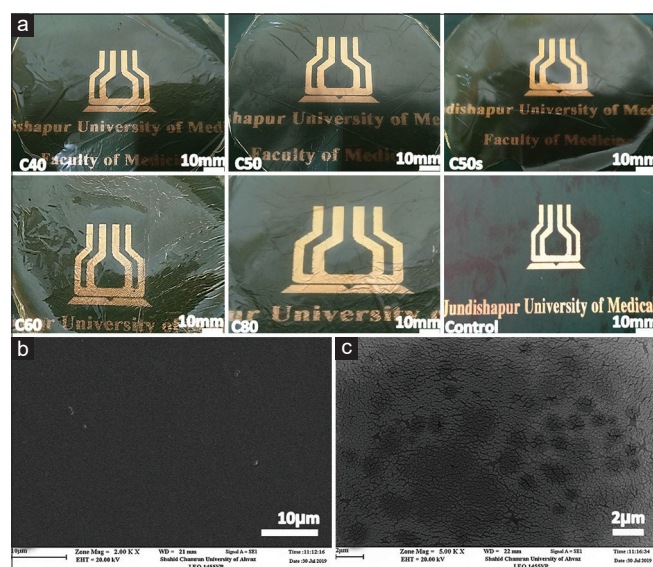


Figure 1: Photographic images of the prepared films and a qualitative assessment of film transparency in comparison with a control image (a). The scanning electron microscopy micrograph of film's surface with two magnifications – $\times 2000$ (b) and $\times 5000$ (c)

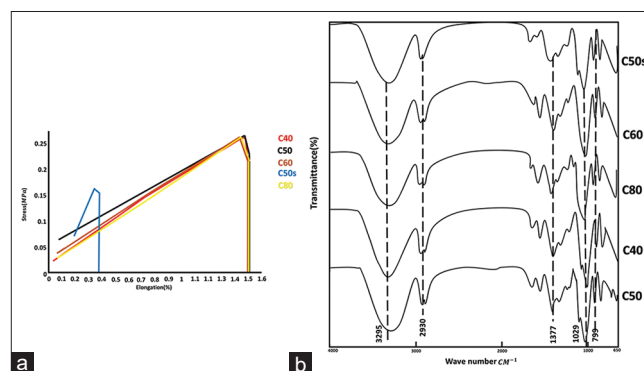


Figure 2: Comparison of mechanical properties of different samples with and without silver nanoparticles (a). Comparison of Fourier transform infrared spectroscopy peaks for different samples along with chemical structure and formula of chitosan and polyvinyl alcohol ($P < 0.05$) (b)

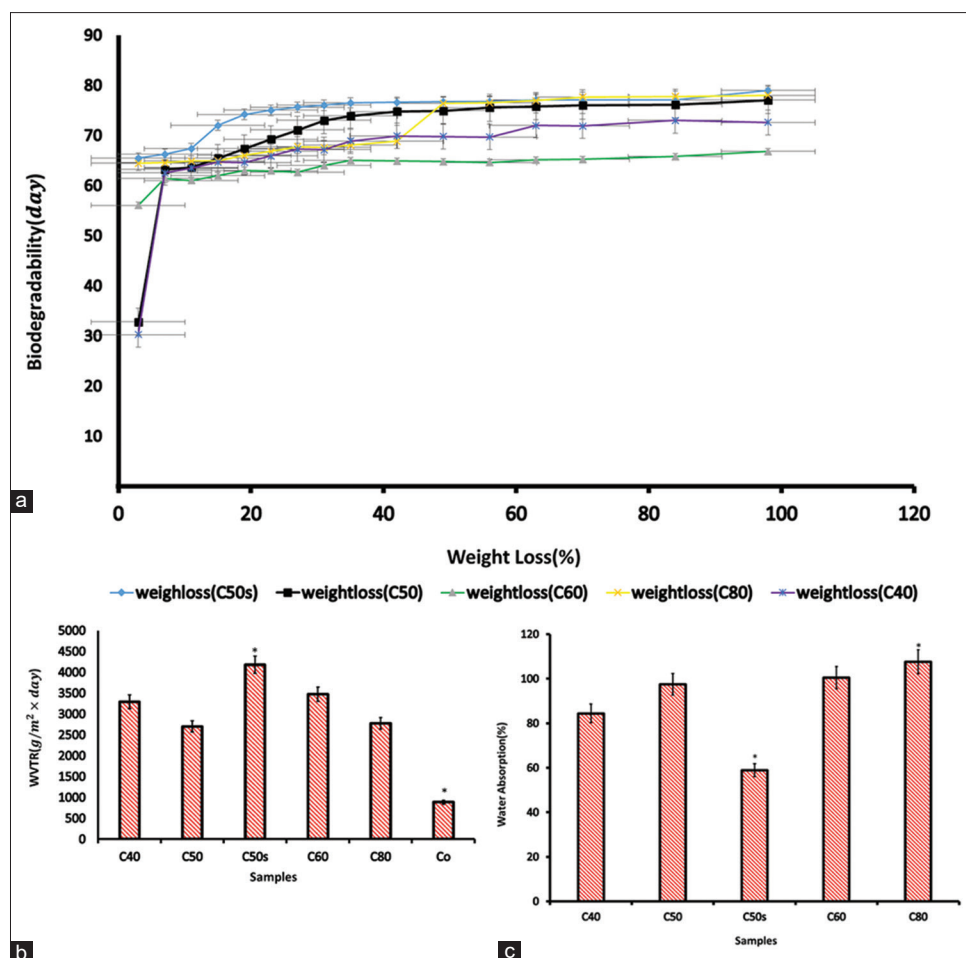


Figure 3: Biodegradability test results for different samples (a). Water vapor transmission rate values for different composite films compared to the control group (b). Percentage of water absorption by different samples of composite films ($P < 0.05$) (c)

Water absorption

The percentage of WA for the samples is displayed in Figure 3c. The percentage of WA increased slightly between samples as the percentage of chitosan increased but decreased significantly with the addition of AgNPs. The C50 sample normally absorbs an amount of water equal to its weight, but the addition of AgNPs reduced its WA rate to 60% of the sample weight.

Cell viability

In the viability test [Figure 4], the mortality rate of implanted cells is high in the 1st to 6th days, and their shape shows a significant decrease when compared to the control group. In all film groups, their viability was significantly higher than that of the control group. Among all groups, the C50s showed the highest viability on the 7th day ($P < 0.05$).

Antibacterial test

The results of the qualitative antibacterial test for the C50s sample disc, which was the film selected for dressing use, are shown in Figure 5b and c depict the ZOI of *B. cereus* (ATCC 27853), and Figure 5d and e represent the ZOI

of *S. aureus* (ATCC 29213), which indicates the intrinsic antibacterial properties of the fabricated dressing.

Discussion

All films were completely transparent, and it was easy to examine the wound healing process without removing them [Figure 1a]. The fabricated dressing had more transparency than dressings used in previous studies.^[21] The smooth, integrated surface of fabricated films at a micrometer scale, in addition to representing the formation of an excellent and homogeneous composite, greatly contributed to the improvement of dressing properties and their ease of use [Figure 1c]. The analysis of mechanical properties [Figure 2a] showed that the mechanical strength of the films was suitable for use as a wound dressing.^[22] However, if the product of this study enters the commercial stage, the strength of silver-loaded films (C50s) should be increased through further researching and testing various materials that might increase the tensile strength of the composite.

In the morphological study of the spectrum of composite materials, it was observed that all the materials used in the

composite film were well combined, but no new chemical bond was formed [Figure 2b].

The biodegradability of the samples decreased with increasing chitosan concentration. Furthermore, the addition of AgNPs (C50s sample) significantly reduced the biodegradability of the film. In wound dressing, less biodegradability is better, as it reduces the absorption of the film skeleton and keeps the dressing firm until the end of the healing process. Applying the optimal WVTR is a crucial parameter of dressings. A very high WVTR causes dehydration and scabbing, while a very low WVTR increases the risk of bacterial infection by increasing the amount of wound secretion [Figure 3a-c]. A desirable WVTR is 2500–3000.^[23] As shown in Figure 3b, the WVTR of the C50 (2702 g/[m² × day]) sample is within this range, but the addition of AgNPs (4179 g/[m² × day]) increased the WVTR by reducing the WA rate of the film. However, both the WA rate [Figure 3c] and the WVTR rate of C50s are acceptable for dressing use.^[16,23]

In the study of human dermal fibroblast (FfK) viability on the sample of fabricated films [Figure 4] from the 1st day to the 6th day, the mortality rate of seeded cells was high, and their shapes indicate a significant decrease when compared to the control group, as the cells are dying due to the stress caused during the passage process and entering the new environment. The doubling time of the fibroblasts used in this experiment was 7 days. On the 7th day, when the cells doubled for the first time after cultivation, the effect of the films on cell growth was better when compared to the control group of the container floor. Furthermore, all samples performed better in cell proliferation on the 7th day. However, the C50s sample was significantly better than the other samples, and so it was selected for use in wound dressings in this study, with all other films excluded. AgNPs, due to their antibacterial potential, are cytotoxic at high doses, though the dose used in this study (2.002 mmole) was not toxic to human fibroblasts. Qualitative analysis of the antibacterial properties of dressings [Figure 5a-d] revealed

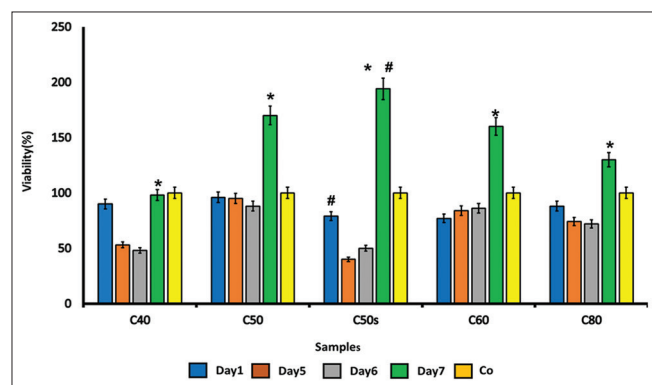


Figure 4: Study of human dermal fibroblast viability on different film samples ($P < 0.05$)

that dressings have clear antibacterial properties for two reasons. The first is the presence of AgNPs; the second is the inherent antibacterial properties of chitosan, which have been well established.^[24]

Compared to other studies, such as temperature-sensitive hydrogel dressing by Dong *et al.*, polycaprolactone electrospun scaffolding and its use in wound healing by Nejaddehbashi *et al.*, and preparation of α -Bisabolol-Loaded Cross-Linked Zein Nanofibrous 3D-Scaffolds and its use in wound healing by El-Lakany *et al.*, the dressing fabricated in the present study performed better and showed better antibacterial properties. The dressing produced in this study was transparent. Further, due to the hydrophilicity of the dressing used in the current study, it is easier to use than other dressings and is less painful to change.^[3,25,26]

Conclusion

In this study, a hydrogel wound dressing loaded with AgNPs was prepared. Hydrogel, which has beneficial WA and moisture retention properties, absorbs wound secretions like a sponge and prevents wound infection, owing to the antibacterial properties of AgNPs. Hydrogel was also found to have good biocompatibility, and it accelerated epithelialization and tissue regeneration in rat wounds by up to a week when compared to other similar dressings. Glycerol/chitosan/PVA hydrogel loaded with AgNPs has promising prospects for wound healing.

Acknowledgment

This work was financial supported by a grant (CMRC-9806) from the vice-chancellor for research affairs of Ahvaz Jundishapur University of Medical Sciences. This study is part of a Ph.D. thesis done by Ali Samadi at Cellular and Molecular Research Center. The authors have no commercial, proprietary, or financial interest in the products or companies described in this manuscript. The authors declare that there is no conflict of interest.

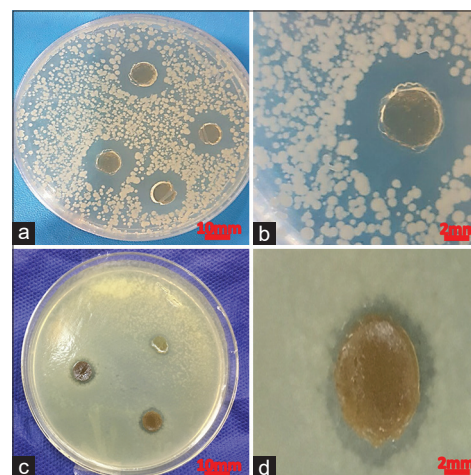


Figure 5: *Bacillus cereus* (a and b) and *Staphylococcus aureus* (c and d)

Financial support and sponsorship

This work was supported by the Deputy of Research of Ahvaz Jundishapur University of Medical Sciences under Grant (CMRC-9806).

Conflicts of interest

There are no conflicts of interest.

References

1. Pawlina W, Ross MH. Histology: A Text and Atlas: With Correlated Cell and Molecular Biology. United States: Lippincott Williams & Wilkins; 2018.
2. Schilling J. Wound Care Made Incredibly Visual. USA: Lippincott Williams & Wilkins; 2007.
3. Nejaddehbashi F, Hashemitabar M, Bayati V, Moghimipour E, Movaffagh J, Orazizadeh M, *et al.* Incorporation of silver sulfadiazine into an electrospun composite of polycaprolactone as an antibacterial scaffold for wound healing in rats. *Cell J* 2020;21:379-90.
4. Marimuthu S, Antonisamy AJ, Malayandi S, Rajendran K, Tsai PC, Pugazhendhi A, *et al.* Silver nanoparticles in dye effluent treatment: A review on synthesis, treatment methods, mechanisms, photocatalytic degradation, toxic effects and mitigation of toxicity. *J Photochem Photobiol B* 2020;205:111-823.
5. Winter GD. Formation of the scab and the rate of epithelization of superficial wounds in the skin of the young domestic pig. *Nature* 1962;193:293-4.
6. Boateng JS, Matthews KH, Stevens HN, Eccleston GM. Wound healing dressings and drug delivery systems: A review. *J Pharm Sci* 2008;97:2892-923.
7. Varaprasad K, Jayaramudu T, Kanikireddy V, Toro C, Sadiku ER. Alginate-based composite materials for wound dressing application: A mini review. *Carbohydr Polym* 2020;236:116-225.
8. Bentoufa S, Miled W, Trad M, Slama RB, Fayala F. Chitosan hydrogel-coated cellulosic fabric for medical end-use: Antibacterial properties, basic mechanical and comfort properties. *Carbohydr Polymers* 2020;227:115-352.
9. He J, Shi M, Liang Y, Guo B. Conductive adhesive self-healing nanocomposite hydrogel wound dressing for photothermal therapy of infected full-thickness skin wounds. *Chem Eng J* 2020;394:124-888.
10. de Lima R, Seabra AB, Durán N. Silver nanoparticles: A brief review of cytotoxicity and genotoxicity of chemically and biogenically synthesized nanoparticles. *J Appl Toxicol* 2012;32:867-79.
11. Rai M, Yadav A, Gade A. Silver nanoparticles as a new generation of antimicrobials. *Biotechnol Adv* 2009;27:76-83.
12. Dahm H. Silver Nanoparticles in Wound Infections: Present Status and Future Prospects. *Nanotechnology in Skin, Soft Tissue, and Bone Infections*. Berlin, Germany: Springer; 2020. p. 151-68.
13. Wichterle O, Lim D. Hydrophilic gels for biological use. *Nature* 1960;185:117-8.
14. Majumder S, Ranjan Dahiya U, Yadav S, Sharma P, Ghosh D, Rao GK, *et al.* Zinc oxide nanoparticles functionalized on hydrogel grafted silk fibroin fabrics as efficient composite dressing. *Biomolecules* 2020;10:710.
15. Kannon GA, Garrett AB. Moist wound healing with occlusive dressings. A clinical review. *Dermatol Surg* 1995;21:583-90.
16. Xu R, Xia H, He W, Li Z, Zhao J, Liu B, *et al.* Controlled water vapor transmission rate promotes wound-healing via wound re-epithelialization and contraction enhancement. *Sci Rep* 2016;6:245-296.
17. Porter JR, Ruckh TT, Popat KC. Bone tissue engineering: A review in bone biomimetics and drug delivery strategies. *Biotechnol Prog* 2009;25:1539-60.
18. Humphries RM, Ambler J, Mitchell SL, Castanheira M, Dingle T, Hindler JA, *et al.* CLSI methods development and standardization working group best practices for evaluation of antimicrobial susceptibility tests. *J Clin Microbiol* 2018;56:e01934-17.
19. Wayne P. Clinical and Laboratory Standards Institute. Performance Standards for Antimicrobial Susceptibility Testing; 2011.
20. Singh B, Pal L. Sterculia crosslinked PVA and PVA-poly(AAm) hydrogel wound dressings for slow drug delivery: Mechanical, mucoadhesive, biocompatible and permeability properties. *J Mech Behav Biomed Mater* 2012;9:9-21.
21. Rafati Z, Sirousazar M, Hassan ZM, Kheiri F. Honey-Loaded Egg White/Poly (vinyl alcohol)/clay bionanocomposite hydrogel wound dressings: *In vitro* and *In vivo* evaluations. *J Polymers Environ* 2020;28:32-46.
22. Jin G, Prabhakaran MP, Ramakrishna S. Stem cell differentiation to epidermal lineages on electrospun nanofibrous substrates for skin tissue engineering. *Acta Biomater* 2011;7:3113-22.
23. Luo Z, Liu J, Lin H, Ren X, Tian H, Liang Y, *et al.* *In situ* fabrication of Nano ZnO/BCM biocomposite based on MA modified bacterial cellulose membrane for antibacterial and wound healing. *Int J Nanomed* 2020;15:1-15.
24. Su Z, Han Q, Zhang F, Meng X, Liu B. Preparation, characterization and antibacterial properties of 6-deoxy-6-arginine modified chitosan. *Carbohydr Polym* 2020;230:115-635.
25. Dong Y, Zhuang H, Hao Y, Zhang L, Yang Q, Liu Y, *et al.* Poly (N-Isopropyl-Acrylamide)/Poly (γ -Glutamic Acid) thermo-sensitive hydrogels loaded with superoxide dismutase for wound dressing application. *Int J Nanomed* 2020;15:1939.
26. El-Lakany SA, Abd-Elhamid AI, Kamoun EA, El-Fakharany EM, Samy WM, Elgindy NA. α -Bisabolol-loaded cross-linked zein nanofibrous 3d-scaffolds for accelerating wound healing and tissue regeneration in rats. *Int J Nanomed* 2019;14:8251.